Studies on Soot Formation and Combustion in Turbulent Spray Flames: Modeling and Experimental Measurement

Bashirnezhad, Kazem
Faculty of Engineering, Islamic Azad University, Mashhad Branch, Mashhad, I.R. IRAN

Moghiman, Mohammad*+; Zahmatkesh, Iman
Faculty of Engineering, Ferdowsi University, Mashhad, I.R. IRAN

ABSTRACT: *The present study is concerned with measuring and simulating soot formation and combustion in turbulent liquid fuel spray flames. Soot concentrations inside the combustor are measured by filter paper technique. The simulation is based on the solution of the fully-coupled conservation equations for turbulent flow, chemical species kinetic modeling, fuel droplet evaporation and combustion and soot formation/oxidation. The soot formation is modeled by using the soot particle number density and the mass density based on acetylene concentrations. Two oxidation models simulate the rate of soot combustion: the O_2-oxidation model, which assumes soot combustion is caused by oxygen molecules, and the O_2-OH oxidation model, which assumes soot combustion occurrs by both hydroxide radicals and oxygen molecules. The experimental and numerical investigations are conducted for different fuel spray cone angles. The comparison of calculated results against experimental measurements shows good agreement. Both the numerical and experimental results show that the peak value of soot and its location in the furnace depend on fuel spray cone angle. An increase in spray angle enhances the evaporating rate and increases peak temperature near the nozzle. The results also show that the OH radical has major influence on soot combustion especially while O_2 oxidation is minimal.*

KEY WORDS: *Soot formation, Soot combustion, Spray angle, Turbulent flames.*

INTRODUCTION

Soot formed during the combustion process has been identified as a serious health risk and a major contributor to global warming. In addition, soot particles significantly enhance radiation heat loss, affecting the performance and durability of many engineering systems such as gas turbines, diesel engines, and industrial combustors. These technological and environmental concerns emphasize the need for innovative methods to design cleaner combustion

** To whom correspondence should be addressed.*
+ E-mail: mmoghiman@yahoo.com
1021-9986/07/3/45 10/$/3.00

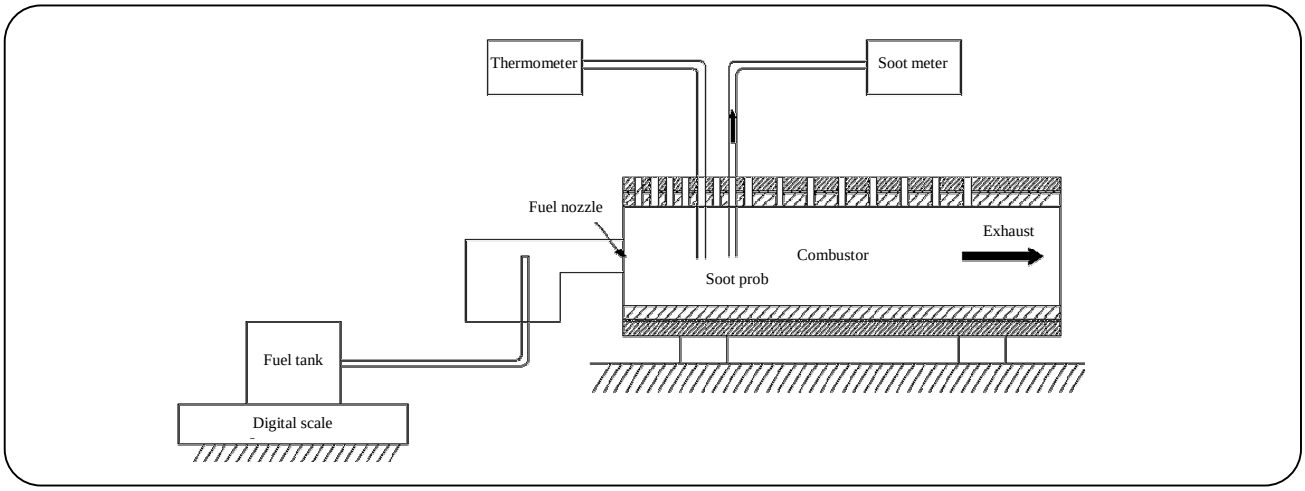

Fig. 1: Schematic view of the experimental set-up.

devices which can ultimately satisfy stricter emission standards for the particulate matters. The effective control of soot emission requires a comprehensive understanding and modeling of the soot formation and oxidation processes that are based on the reliable measurements within well-defined flames [1].

The process of soot production from hydrocarbon fuels consists of complex chemical and physical steps, including fuel pyrolysis, formation of polycyclic aromatic hydrocarbons, particle inception, coagulation, surface growth and combustion [2]. Kinetic studies of different workers reveal a dominant kinetic pattern of aromatic-ring growth, H-abstraction and C_2H_2- addition [3]. The soot formation model employed in this study is based on the assumption that soot inception and surface growth is a first order function of acetylene concentration. The successful modeling of soot yield also depends on soot combustion model. The OH radical and molecular oxygen O_2 are the most important species in soot oxidation according to *Brookes* and *Moss* [4]. More direct measurements have indicated that OH is an important oxidant of soot especially in the regions of diffusion flames where O_2 oxidation is minimal [5].

Typically, flames of liquid fuels have greater soot emission than the gaseous fuels, which is a direct result of diffusion character of these types of flames. Therefore, soot process in this type of flames should be considered more precisely. However, soot processes in spray flames are closely related to atomization, penetration, heating up, and evaporation of droplets which make the study of spray flames a challenging task according to *Sommerfeld et al.* [6] and *Moghiman* [7]. The detailed modeling of the chemistry and physics of soot formation and oxidation in turbulent combustion systems is strongly sensitive to atomization parameters.

The aim of this paper is the study of soot formation and oxidation in turbulent liquid fuel spray flames using both modeling and experimental measurements. The soot formation is modeled by two parameters, the number density of the particle (N) and the mass density (M). The nucleation and surface growth rate for soot particles are taken to be proportional to the local acetylene concentration. Two different soot oxidation models are implemented and the results are compared with each other and with the experimental measurements. The experimental measurements and numerical predictions are conducted under different fuel spray cone angles.

EXPERIMENTAL SET-UP

A full-scale horizontal laboratory combustor with a circular cross-section made of AISI 316 stainless steel is constructed to confine the flame and prevent gas composition fluctuations from the ambient air. The full-scale combustor is 360 mm in diameter and 1000 mm in length, that ensures that the essential physics of full-scale combustor are simulated. An oil burner atomizes the pressurized fuel oil inside the combustor. A schematic diagram of the experimental set-up is illustrated in Fig. 1.

Some rectangular slots are cut into the upper side of the combustor body so that the soot meter and thermocouple probes can be inserted into the center of the cylindrical combustor. Soot concentration is measured

using the filter paper technique [8]. The temperature inside the combustor is measured using the ceramic-sheathed type S-thermocouples with a resistance temperature up to 2000 K. The described system measures temperatures within a tolerance of 1 K. Mass flow rate of the fuel is measured by using an analytical scale with the accuracy of 1g. The air into the burner is metered by a rotameter. The temperature of the fuel is maintained at 323 K using an electric heating element. The temperature fluctuation of the inlet air and fuel is kept within the specified margins of 4 K. The repeatability of the data is regularly checked during each experimental session. On average, all of the data can be reproduced to within 10% of the mean value. The combustor flow-gas is continuously monitored during the measurement program to sense any change in the combustor operating conditions. In addition, although every effort is made to eliminate sources of gas leakage in the combustor construction, the combustor pressure is maintained close to atmospheric.

NUMERICAL SIMULATION

Basic assumptions

In this study, the following basic assumptions are made to produce a mathematical model for various processes inside the combustor:

- We consider that a axisymmetric two-dimensional computational fluid dynamics analysis of a turbulent diffusion flame is able to predict gas velocity, temperature and 84 species concentration profiles with sufficient accuracy.
- The fuel spray is considered to consist of a finite size range, with the size distribution specified by the *Rosin-Rammler* function.
- A one-way interaction model is used for the gas flow and the droplets trajectory analysis. That is, it is assumed that air carries the droplets, but they have no effect on the air flow.
- The soot particle phase is considered to be dilute and is considered not to affect the gas flow field.
- Buoyancy forces are neglected.
- The liquid fuel is considered to be kerosene.

Mathematical model

The mathematical model is based on a typical Eulerian gas phase and a Lagrangian droplet phase formulation. Since a one-way interaction model is used for the gas flow and the droplets trajectory analysis, the air flowfield is firstly evaluated while the results are used for evaluation of the droplets trajectories.

Gas phase conservation equations

The time averaged gas phase equations are as follows:

Continuity and Momentum

$$\frac{\partial u}{\partial x}+\frac{1}{r}\frac{\partial}{\partial r}(rv)=\dot{S} \tag{1}$$

$$\frac{1}{r}\left[\frac{\partial}{\partial x}(r\rho uu)+\frac{\partial}{\partial r}(r\rho uv)\right]=-\frac{\partial p}{\partial x} \tag{2}$$

$$+\mu\nabla^2 u-\frac{1}{r}\frac{\partial}{\partial r}(r\rho\overline{u'v'})-\frac{\partial}{\partial x}(\rho\overline{u'u'})$$

$$\frac{1}{r}\left[\frac{\partial}{\partial x}(r\rho uv)+\frac{\partial}{\partial r}(r\rho vv)-\rho w^2\right]= \tag{3}$$

$$-\frac{\partial p}{\partial r}+\mu(\nabla^2 v+\frac{v}{r^2})-\frac{1}{r}\frac{\partial}{\partial r}(r\rho\overline{v'v'})-$$

$$\frac{\partial}{\partial x}(\rho\overline{u'v'})-\frac{1}{r}\rho\overline{w'w'}$$

$$\frac{1}{r}\left[\frac{\partial}{\partial x}(r\rho uw)+\frac{\partial}{\partial r}(r\rho vw)+\rho vw\right]= \tag{4}$$

$$\mu(\nabla^2 w-\frac{w}{r^2})-\frac{1}{r}\frac{\partial}{\partial r}(r\rho\overline{v'w'})-$$

$$\frac{\partial}{\partial x}(\rho\overline{u'w'})-\frac{1}{r}\rho\overline{v'w'}$$

where source term is represented by $\dot{S}$ arising from the mass interaction between gas and droplets. In the view of inability of the k-ε model to cope with anisotropic flows according to *German* and *Mahmud* [9], the turbulent stresses are calculated from an algebraic stress model [10]. In addition, a conventional wall-function approach is used in the near-wall region to bridge the viscous sublayer.

Energy

$$\frac{1}{r}\left[\frac{\partial}{\partial x}(r\rho uh)+\frac{\partial}{\partial x}(r\rho vh)\right]=\Gamma_h\nabla^2 h \tag{5}$$

$$-\frac{1}{r}\frac{\partial}{\partial r}(r\rho\overline{v'h'})-\frac{\partial}{\partial x}(\rho\overline{u'h'})+\dot{S}_h$$

The energy source term ($\dot{S}_h$) is the energy generated due to chemical reaction. The energy addition due to combustion is determined in consideration of a detailed chemical kinetic mechanism with 84 species and 440 elemental reactions as proposed by *Patterson et al.* [11]. In this study, the reaction rates that appear as source terms in species transport equations (Eq. (8)) are controlled by an *Arrhenius* kinetic rate expression. The *Arrhenius* reaction rate for species α in the k-th reaction ($R_{\alpha,k}$) is calculated from *Westbrook* and *Dryer* [12], as:

$$R_{\alpha,k} = \left(\nu''_{\alpha,k} - \nu'_{\alpha,k}\right) k_k \prod_{j=1}^{84} \left(C_j\right)^{\nu'_j} \quad (6)$$

where $\nu'_{\alpha,k}$ is the stoichiometric coefficient of reactant α in reaction k, $\nu''_{\alpha,k}$ is the stoichiometric coefficient of product α in reaction k, k_k is the reaction rate coefficient in reaction k and C_j is the molar concentration of each reactant or product species j. The gas phase equations are completed by the ideal equation of state, which determines the distribution of density as:

$$\rho = \frac{P}{RT}\left[\sum \frac{m_j}{M_j}\right] \quad (7)$$

This assumption is appropriate since the high temperatures associated with combustion generally results in sufficiently low densities, for ideal gas behavior to be a reasonable approximation.

Individual species conservation

$$\frac{1}{r}\left[\frac{\partial}{\partial x}(r\rho u m_j) + \frac{\partial}{\partial r}(r\rho v m_j)\right] = \Gamma_{mj}\nabla^2 m_j - \frac{1}{r}\frac{\partial}{\partial r}(r\rho\overline{v'm_j'}) - \frac{\partial}{\partial x}(\rho\overline{u'm_j'}) + R_j + S_j \quad (8)$$

where, R_j is the mass rate of reaction or depletion by gas-phase chemical reactions, S_j is the rate of creation by vaporization occurring on the surface of the individual droplets and Γ_{mj} is the laminar exchange coefficient. In this study, species conservation equation is solved for all of the 84 species.

Generation of droplet phase information

The velocity, mass and temperature history of all droplet groups along their trajectories are obtained from the respective conservation equations on a Lagrangian frame similar to *Sharma* and *Dom* [13]. The range of droplet size is considered to be in the range of 10 to 100μm to be consistent with the experiment, ten droplet group sizes are assumed in this range and calculation is performed for each of the droplet sizes according to *Faeth* [14].

Soot modeling

The emission of soot from a flame is determined by a competition between soot formation and oxidation that must be considered when a soot modeling study is carried on. In this study, a recent soot model developed by *Moss et al.* [15], is used. The model describes the soot formation in terms of the soot particle number density (N) and the soot particle mass density (M) and takes into account the inception (nucleation), coagulation, growth and oxidation processes for the rates of these two model parameters as:

$$\frac{DN}{Dt} = \left(\frac{dN}{dt}\right)_{Inception} + \left(\frac{dN}{dt}\right)_{Coagulation} \quad (9)$$

$$\frac{DM}{DT} = \left(\frac{dM}{dt}\right)_{Inception} + \left(\frac{dM}{dt}\right)_{Growth} + \left(\frac{dM}{dt}\right)_{Oxidation} \quad (10)$$

The acetylene inception model is used for the calculation of soot inception rate according to *Brookes* and *Moss*, [4], and *Lueng et al.* [16].

Taking into account that presence of aromatics in kerosene enhances inception, the inception rates are computed by:

$$\left(\frac{dN}{dt}\right)_{Inception} = c_1 N_A \left(\rho \frac{m_{C_2H_2}}{W_{C_2H_2}}\right) e^{-21100/T} \quad (11)$$

$$\left(\frac{dM}{dt}\right)_{Inception} = \frac{M_P}{N_A}\left(\frac{dM}{dt}\right)_{Inception} \quad (12)$$

where M_p, the mass of a soot nucleus, has a value of 144 kg $kmol^{-1}$ based on the assumption that the soot size corresponds to 12 carbon atoms and c_1 =54 s^{-1} determined by *Brookes* and *Moss* [4].

Assuming the particles are mono-dispersed in size and spherical, the coagulation rate and reaction surface are given by:

$$\left(\frac{dN}{dt}\right)_{Coagulation} = -\left(\frac{24R}{\rho_{Soot} N_A}\right)^{1/2} \times \left(\frac{6}{\pi\rho_{Soot}}\right)^{1/6} T^{1/2} M^{1/6} N^{11/6} \quad (13)$$

$$\left(\frac{dM}{dt}\right)_{growth} = c_2 \left(\rho \frac{m_{C_2H_2}}{W_{C_2H_2}}\right) e^{-21100/T} \times \left((\pi N)^{1/3} \left(\frac{6M}{\rho_{Soot}}\right)^{2/3}\right) \quad (14)$$

where R is the universal gas constant, ρ_{soot}=2000 kgm^{-3} and c_2 =9000.6 kg m kmol^{-1} s^{-1} according to ***Wen et al.*** [17].

To predict soot oxidation two combustion models are used. The first model is the model proposed by ***Lee et al.*** [18]. This model considers O_2 as the dominant contributor to soot oxidation and thus is referred to as the O_2-oxidation model. In this model, the rate of soot oxidation is given by,

$$\left(\frac{dM}{dt}\right)_{Oxidation} = C_3 \rho \frac{m_{O_2}}{W_{O_2}} Exp\left(\frac{-19778}{T}\right) \sqrt{T} (\pi N)^{1/3} \left(\frac{6M}{\rho_{Soot}}\right)^{2/3} \quad (15)$$

where c_3 = 8903.51 kg m kmol^{-1} K$^{-1/2}$ [19].

The second model takes into account oxidation of soot both by O_2 and OH radicals and is referred to as the O_2-OH oxidation model. In this model, the rate of soot oxidation is given by:

$$\left(\frac{dM}{dt}\right)_{Oxidation} = -c_4 \rho \eta \frac{m_{OH}}{W_{OH}} \sqrt{T} (\pi N)^{1/3} \left(\frac{6M}{\rho s}\right)^{2/3} \times - c_3 \rho \frac{m_{O_2}}{W_{O_2}} Exp\left(\frac{-19778}{T}\right) \sqrt{T} (\pi N)^{1/3} \left(\frac{6M}{\rho_{Soot}}\right)^{2/3} \quad (16)$$

where η is set to be 0.13, c_4 =105.81 kg m kmol^{-1} K$^{-1/2}$ s^{-1}, which are obtained by converting the rate of soot mass consumption [17].

METHOD OF SOLUTION

Numerical scheme

The gas conservation equations are solved using a control-volume based computational procedure [20]. The convective terms are discretized by the power law scheme. The flow field pressure linked equations are solved by the SIMPLE algorithm and the set of algebraic equations are solved sequentially with the line-by-line method which is a combustion of *Gauss-Seidel* method and tridiagonal-matrix algorithm. The convergence criterion is determined by the requirement that the maximum value of the normalized residuals of any equation must be less than 1×10^{-5}. Under-relaxation factor is chosen as 0.3 for all dependent variables.

Numerical mesh

A numerical mesh of 240×120 grid nodes is used after several experiments, which shows that further refinement in either direction does not change the result (maximum difference in velocity and other scalar functions in the carrier phase) by more than 2%. The grid spacing in axial and radial directions are changed smoothly to minimize the deterioration of the formal accuracy of the discretization scheme due to variable grid spacing and in such a way that higher concentration of nodes occur near the inlet and the walls.

Operating parameters and boundary conditions

Because of elliptic nature of the conservation equations, boundary conditions are specified at all boundaries of the domain considered. The air enters the combustor with the temperatures of 298 K and with the axial velocity of 3 m/s. Mass flow-rate of the liquid fuel, which is injected at 323 K, equals to 0.05 kg/s while different spray cone angles are investigated. In addition, at the outlet, for all variables, a zero axial gradient is prescribed.

RESULTS AND DISSCUSSION

Fig. 2 displays the distribution of predicted stream function contours of the gas phase within the combustor for the specified condition from the solution of the present numerical model. It is observed that due to a sudden expansion at the inlet of the combustor a corner recirculation zone establishes near the cylindrical wall. The recirculation zone can affect the mixing process in the vicinity of the point of the issue.

In spray flames, an important parameter which has a profound effect on the evaporation and mixing rates, is the fuel spray cone angle. Fig. 3 shows measured and

predicted centerline temperature profiles for three fuel spray cone angles using O_2-OH soot oxidation model. It is seen that the agreement between predicted and measured data is very good. Comparison of the results of the three-fuel spray cone angles reveals that an increase in fuel spray cone angle increases the combustor centerline temperature levels. This is due to the increased size ofspray cone zone and increased mixing rates between the fuel droplets and the oxidant.

The species C_2H_2 is the most important precursor of soot formation and the formation of C_2H_2 strongly depends upon the fuel concentration and temperature [15]. Fig. 4 shows the centerline C_2H_2 distribution for three spray cone angles. It can be seen that as expected, the location of C_2H_2 maximum values are in the vicinity of the nozzle where fuel concentration and temperature levels are high (see Fig. 3). Note that region with the highest C_2H_2 mass fraction is not located in the region with highest temperature and this is in accord with the result of *Wen et al.* [17]. The comparison of the results of three spray cone angles shows that an increase in spray cone angle increases C_2H_2 mass fraction especially close to fuel spray nozzle. This is due to the increase in the surface between air and fuel that provides good fuel evaporation.

Measurements of the soot volume fraction distribution inside the combustor with three fuel spray cone angles (30º, 45º and 60º) are shown in Fig. 5. It can be seen that the maximum soot volume fraction occurs in the vicinity of the fuel injection point where the fuel concentration and temperature levels are high (see Fig. 3). This occurs because the process of soot nucleation and surface growth are strongly temperature and fuel concentration dependent. The comparison of the results of the three fuel spray angles reveals that an increase in the fuel spray cone angle increases the soot volume fraction levels near the nozzle. The fuel injected from lower spray angle penetrates longer axial distance into the gas flow and produces higher soot volume fraction near the outlet of the combustor.

Predictions of the soot volume fraction distributions inside the combustor for three fuel spray cone angles (30º, 45º and 60º) are shown in Fig. 6. The calculation of soot formation is based on the assumption that nucleation and growth processes are acetylene concentration dependent and soot oxidation is based on O_2-OH

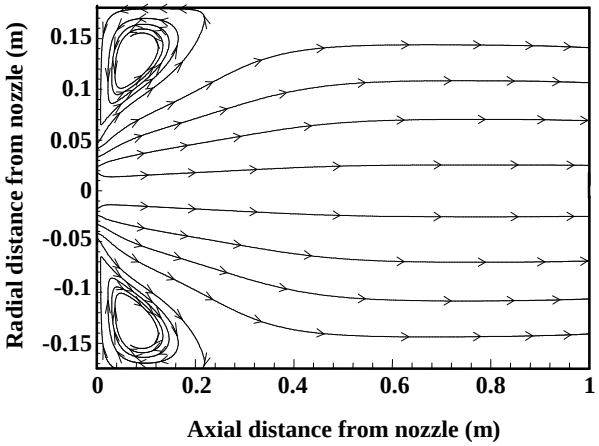

Fig. 2: Predicted gas phase stream line distribution.

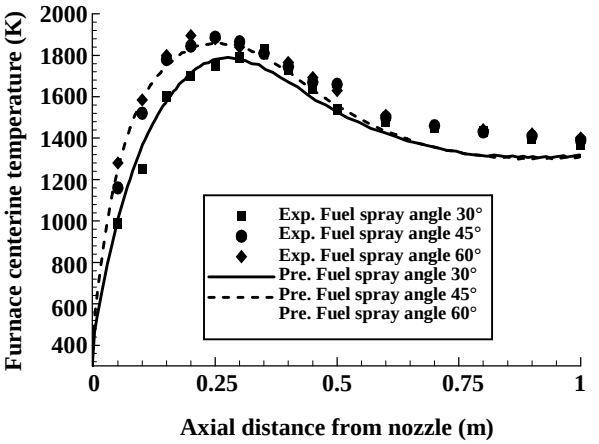

Fig. 3: Effect of spray cone angles on centerline temperature distribution.

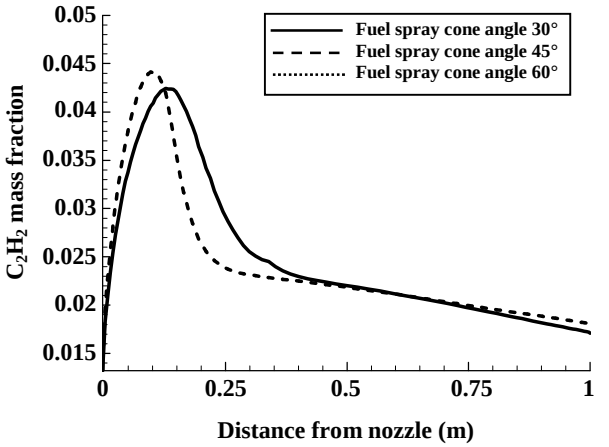

Fig. 4: Effect of spray cone angles on centerline C_2H_2 distribution predictions.

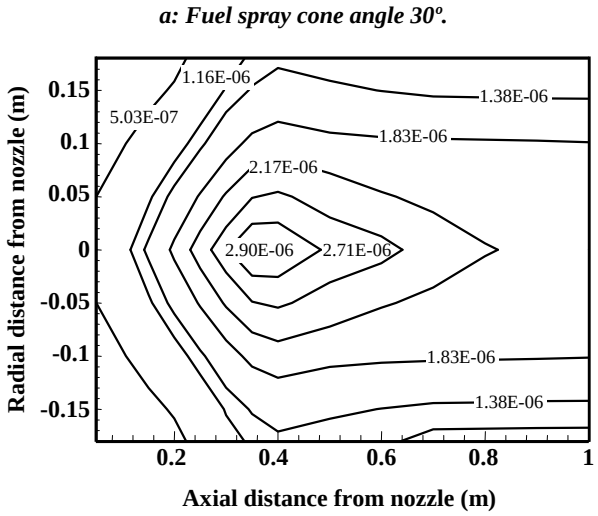

Fig. 5: Measured soot volume fraction distributions inside the combustor for different fuel spray angles.

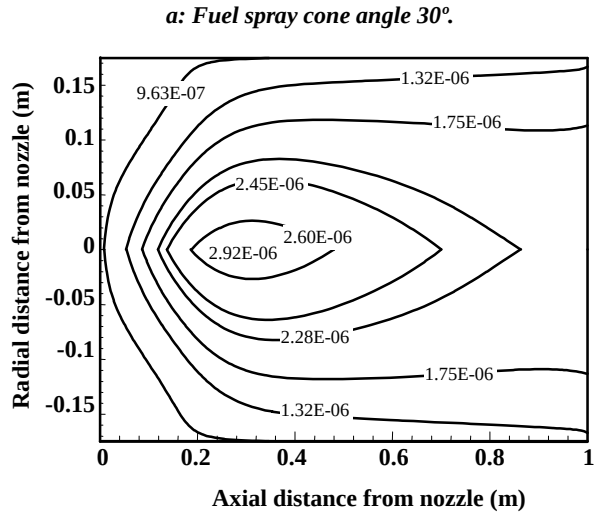

Fig. 6: Predicted soot volume fraction distributions inside the combustor for different fuel spray angles(O_2-OH oxidation model).

a: Fuel spray cone angle 30º.

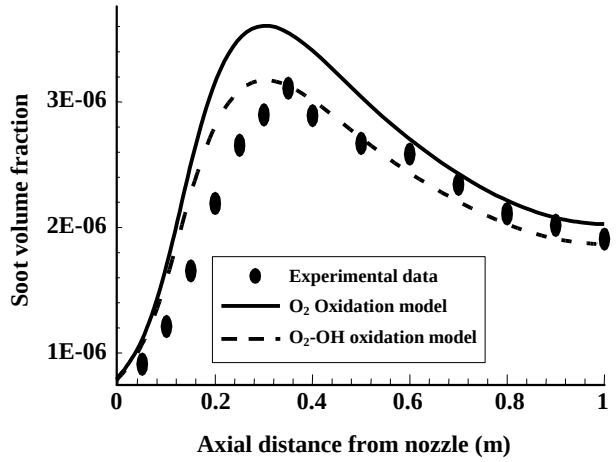

b: Fuel spray cone angle 45º.

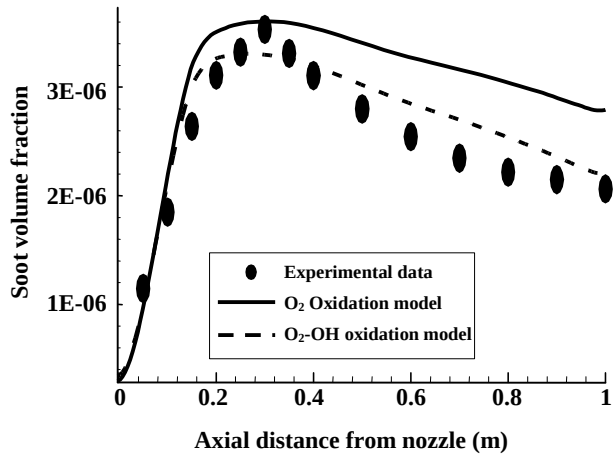

c: Fuel spray cone angle 60º.

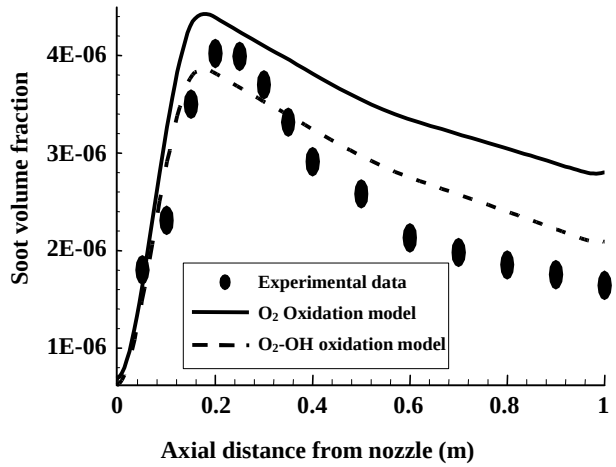

Fig. 7: Comparison between the centerline soot volume fractions of the two soot oxidation models with the experimental data.

concentration. The prediction results have a good agreement with the experimental data (see Fig. 5).

More detailed comparison of measured and predicted soot volume fractions are given in Fig. 7 where centerline profiles of two soot oxidation models are compared with experimental measurements for three spray cone angles. The comparison between the computed results of the two soot oxidation models with experimental data shows that O_2-OH oxidation model predicts more correctly. This occurs because in this model the oxidation of soot is a result of an attack by both molecular oxygen O_2 and OH radicals. As oxygen is consumed rapidly in the vicinity of the inlet port, OH-radical is an important oxidant along the combustor where O_2 concentration is minimal.

Fig. 8 shows the effect of spray cone angle on centerline OH mass fractions. The influence of spray angle on OH mass fractions is indicated by reference to Fig. 3 where centerline temperature levels of the three spray angles are shown. It can be seen that OH mass fraction is strongly temperature dependent. This is in accord with the experimental measurements of *Bradley et al.* [21].

CONCLUSIONS

In this study, experimental measurements and numerical simulations of soot formation/combustion in turbulent spray flames are carried out for different fuel spray cone angles. Soot concentrations inside the combustor are measured by filter paper technique. Soot inception and surface growth are modeled through acetylene concentration. Also, the effect of two soot combustion models, the O_2-oxidation model and the O_2-OH oxidation model, are investigated. Comparison of experimentally measured soot concentrations and temperature levels with computed results shows that the numerical method with a O_2-OH soot oxidation model is a useful tool for predicting soot formation/combustion in turbulent spray flames. Based on the presented results, the following conclusions can be drawn:

- Spray cone angle has a significant influence on C_2H_2 and soot concentrations especially in the vicinity of the combustor nozzle.

- In the vicinity of the point of the issue, due to evaporation of the injected fuel and a high temperature level, a peak in the soot volume fraction occurs.

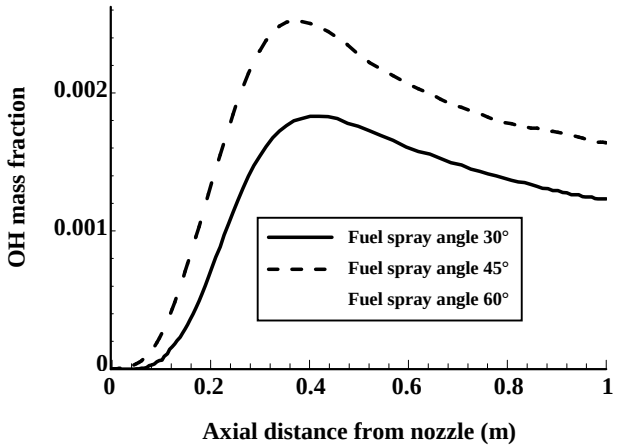

Fig. 8: Centerline distribution of predicted OH mass fractions.

- Although an increase in fuel spray angle increases the maximum value of soot concentration in the vicinity of the point of the issue, soot emission decreases from the combustor due to the increased mixing rates between soot particles and oxidant.

- The O_2 and OH concentrations play important roles on soot combustion in liquid/air diffusion flames and OH radical dominates soot combustion while O_2 combustion is minimal.

Nomenclatures

c_1	Scaling factor for the soot inception model
c_2	Scaling factor for the soot growth
c_3	Scaling factor for O_2 oxidation rate
c_4	Scaling factor for OH oxidation rate
c_p	Specific heat
$m_{F,s}$	Fuel vapor mass fraction at the particle surface
d	Droplet diameter
D_{eff}	Effective mass diffusivity
h	Enthalpy
m	Mass fraction
M	Soot mass density
N	Soot particle number density
N_A	Avogadro's number
Pr	Prandtl number
r	Radial direction
R	Universal gas constant
Sw	Swirl number
$\dot{S}$	Gas phase mass source term due to evaporation of fuel droplets
$\dot{S}_j$	Species conservation equation source term of the j th specie
$\dot{S}_h$	Gas phase energy conservation equation source term
T	Mean temperature
u	Axial velocity component
v	Radial velocity component
w	Swirl velocity
W	Molecular weight
x	Axial direction

Greek letters

α_{eff}	Effective thermal diffusivity
μ	Molecular viscosity
ρ	Gas phase density
η	Collisional efficiency of soot particles

Superscript

d	Droplet
g	Gas phase

Received : 3rd March 2006 ; Accepted : 30th October 2006

REFERENCES

[1] Gruenberger, T.M., Moghiman, M., Bowen, P.J. and Syred, N., *Journal of Comb. Sci. Tech*., **174**, 67 (2002).

[2] Yang, B. and Koylu, U.O., *Journal of Comb. Flame,* **141**, 55 (2005).

[3] Roesler, J.F., Martinot, S., McEnally, C. S., Pfefferle, L. D., Delfau, J. L. and Vovelle, C., *Journal of Comb. Flame*, **134**, 249 (2003).

[4] Brookes, S. J. and Moss, J. B., *Journal of Comb. Flame,* **116**, 486 (1999).

[5] Beltrame, A., Porshnev, P., Merchan-Merchan, W., Saveliev, A., Fridman, A., Kennedy, L.A., Petrova, O., Zhdanok, S., Amouri, F. and Charon, O, *Journal of Comb. Flame*, **124**, 295 (2001).

[6] Sommerfeld, M. and Qiu, H. H., *Journal of Heat Fluid Flow*, **19**, 10 (1998).

[7] Moghiman, M. and Maneshkarimi, M. R., *Iranian Journal Sci. Tech.,* **25**, 241 (2001).

[8] AVL Smoke Measurement, *AVL LIST GMBH, Graz* (2001).

[9] German, A.E. and Mahmud, T., *Journal of Fuel*, **84**, 583 (2005).
[10] Zhang, J., Nieh, S. and Zhou, L., *Journal of Numerical Heat Transfer*, **22**, 49 (1992).
[11] Patterson, P.M., Kyne, A.G., Pourkashanian, M., Williams, A. and Wilson, C.W., **6**, 453 (2001).
[12] Westbrook, C.K. and Dryer, F.L., *Journal of Comb. Sci. Tech.*, **27**, 31 (1981).
[13] Sharma, N.Y. and Dom, S. K., *Journal of Applied Thermal Eng.*, **24**, 885, (2004).
[14] Faeth, G.M., *Journal of Prog. Energy Comb. Sci.*, **9**, 16 (1983).
[15] Moss, J.B., Stewart, C.D. and Young, K.J., *Journal of Comb. Flame*, **101**, 491 (1995).
[16] Lueng, K. M, Lindstedt, R. P. and Jones, W. P., *Journal of Comb. Flame*, **87**, 289 (1991).
[17] Wen, Z., Yun, S., Thomson, M.J. and Lightstone, M.F., *Journal of Comb. Flame*, **135**, 323 (2003).
[18] Lee, K.B., Thring, M.W. and Beer. J.M., *Journal of Comb. Flame*, **6**, 137 (1962).
[19] Lindstedt P.R., "Soot Formation in Combustion", pp. 417-441, Springer-Verlag, Berlin (1994).
[20] Versteeg, H. K. and Malalaseke, W., "An Introduction to Computational Fluid Dynamics-The Finite Volume Method", Longman Scientific & Technical (1996).
[21] Bradley, D., Dixon-Lewis, G., Habik, S. and Mushi, E.M., Twentieth Symposium (International) on Combustion, The Combustion Institute, Pittsburgh, Pennsylvania, USA (1984).